Materials and Structures (2015) 48:557–569
DOI 10.1617/s11527-014-0432-2

ORIGINAL ARTICLE

FT-IR and ^{29}Si-NMR for evaluating aluminium–silicate precursors for geopolymers

Siska L. A. Valcke · Panagiota Pipilikaki · Hartmut R. Fischer · Margriet H. W. Verkuijlen · Ernst R. H. van Eck

Received: 30 May 2014 / Accepted: 26 September 2014 / Published online: 30 October 2014

Abstract Geopolymers are systems of inorganic binders that can be used for sustainable, cementless concrete and are formed by alkali activation of an aluminium–silicate precursor (often secondary resources like fly ash or slag). The type of aluminium–silicate precursor and its potential variations within one batch may influence geopolymer performance. Therefore, if geopolymers are to be applied for sustainable concrete with reproducible quality, a characterization tool for quality control of precursors and optimizing mix design is needed, which links the (variable) secondary resource characteristics to the performance of geopolymers. This paper shows the potential of using FT-IR and solid state ^{29}Si-NMR for a (semi-)quantitative evaluation of secondary resources suitable for geopolymers. More specifically, the aim is to investigate whether the presence of particular aluminium–silicate phases may have a dominant influence on the strength of a simple geopolymer system. Based on deconvolution of FT-IR and NMR spectra of 9 source materials (fly ash and slag) and their geopolymers, relative amounts of different (aluminium–silicate) phases were estimated and trends with strength were evaluated. A clear trend is observed for both NMR and FT-IR results: the precursors containing a higher amount of 'active bonds', predominantly from silicates with a medium amount of aluminium and alkalis incorporated in their framework, result in higher paste strengths. As such, due to its relatively quick and easy measurements, FT-IR for estimating relative amounts of these aluminium–silicate phases, can be a useful tool for evaluating geopolymer precursors.

Keywords FT-IR · Solid state ^{29}Si-NMR · Geopolymer · Secondary resources · Fly ash · Blast furnace slag · Sustainable concrete

S. L. A. Valcke (✉) · P. Pipilikaki · H. R. Fischer
Structural Reliability, Netherlands Organisation for Applied Scientific Research TNO, Delft, The Netherlands
e-mail: siska.valcke@tno.nl

M. H. W. Verkuijlen · E. R. H. van Eck
Institute for Molecules and Materials, Radboud University Nijmegen, Nijmegen, The Netherlands

1 Introduction

Driven by the increased demand for sustainable products and solutions, novel technologies have been developed in the past decades for the realization of sustainable concrete at reduced primary (energy) use and lower CO_2 emissions. Geopolymers are systems of inorganic binder that can be used for cementless low CO_2 concrete and consist of an aluminium–silicate precursor with an alkali activating solution. The aluminium–silicate precursors are very often secondary resource materials such as combustion products (fly ash, bottom ash), blast furnace slag etc. [4, 18].

Although the debate on their sustainability is still ongoing, in the meantime, research, demonstrations and small scale plants have shown that geopolymers also

open pathways for tailor made concrete having unique properties different to traditional cement concrete (improved fire resistance, improved insulation etc.) [23]. If geopolymers are to be used for sustainable concrete or other innovative products, tools are needed to assess potential variations in secondary resources that can affect geopolymer performance. Therefore, an evaluation tool for linking the secondary resource characteristics to the performance of geopolymers would prove very useful. For this, particularly those secondary resource characteristics that have a dominant influence on the ability of source materials to react and form a strong binder product need to be investigated. Source material characteristics that have been stated in the literature to influence their potential for geopolymerization, include: amount of soluble silicon and aluminium (directly related to amorphous glass content), content of network modifying ions (calcium, iron, sodium,..), crystallinity, particle shape and size [3, 5, 6, 8, 12, 24–26]. Provis and van Deventer [16, 17] have shown that the Si:Al ratio of the source material plays a major role in the geopolymerisation process, not only in the early dissolution rate, but also in gelation and precipitation rates. Also, in other papers it has been shown that Si:Al ratio seems a more dominant key variable than for example particle size [12, 24]. Nevertheless, the relation between bulk Si:Al ratio and geopolymer performance (strength) is not straightforward due to heterogeneities in the phases that contain aluminium and silicon. Aluminium and silicon in the source material are incorporated in quartz as well as in glassy and crystalline aluminium–silicates, but it is only the glassy aluminium–silicates that are reactive and even within the latter, variations in aluminium:silicon ratio occur which may influence strength [12, 24].

For directly evaluating and comparing different types of (reactive) aluminium–silicates in precursors and their corresponding geopolymers, FT-IR and solid state ^{29}Si-NMR have been used in previous studies [1, 7, 15, 19]. This was mostly done qualitatively, but in a few papers, FT-IR and NMR spectra were deconvolved for (semi-) quantitatively evaluating the type of aluminium–silicate phases in geopolymer (precursors). In Fernández-Jiménez et al. [9] the relation between different aluminium–silicate types in the gel stage and geopolymer strength is investigated for three fly ash types using deconvolution of NMR spectra. The influence of mix design parameters and precursors on the silicate structures formed during geopolymerization is investigated by Criado et al. [5] using deconvolution of FT-IR spectra. Zhang et al. [26] have shown a relation between type of chemical bonds in the precursors and geopolymer strength using deconvolution of FT-IR spectra.

The aim of the current paper is to build further on these studies and to combine both insights from (semi-)quantitative NMR on the amount of aluminium incorporated in the silicates as well as from (semi-)quantitative FT-IR on the type of reactive bonds in the precursors, in order to investigate the potential of a simple evaluation tool for precursors using (semi-)quantitative FT-IR.

2 Materials

For investigating the influence of geopolymer precursor characteristics on strength, a significant spread in 9 source materials was chosen: 6 fly ashes (F1–F4, F6–F7) of the siliceous F-type but with a different Si:Al ratio and 1 fly ash (F5) containing more than twice as much calcium (CaO $>$ 13.74 %) as the other fly ashes (Table 1). The fly ash samples (F1–F7) are from seven different sources of coal-fired steam power plants in Europe (The Netherlands, Greece, United Kingdom). Additionally, two ground granulated blast furnace slag samples from two different sources of iron-producing blast furnaces in Europe were used (S1 & S2, Table 1). The chemical XRF data of the samples given in Table 1 are taken from Barnett et al. [2] and S&B Industrial Minerals [20]. The fly ash and slag samples from the UK (F6–7, S1–S2) were selected based on the work described in Barnett et al. [2].

In order to minimize variables influencing strength, simple geopolymer pastes are made (Table 1), solely by activation with NaOH. It is hereby acknowledged that NaOH does not necessarily produce the strongest geopolymers, but the aim here is to investigate what the potential is of the aluminium–silicates solely coming from the source materials, without the influence of silicates of for example waterglass based activators.

Concerning the mix design the following approach is taken. Due to the source material's chemical and morphological differences and their subsequently substantially different water absorption, it is not possible to keep the water:binder ratio of the mix constant without changing the *effective* water/binder ratio and the rheology of the samples, both affecting strength development. Therefore it was chosen to design pastes using constant slump and constant NaOH concentration

Table 1 Table showing general bulk characteristics

Source material				
Code	Si:Al (XRF)[a]	CaO (XRF)[a]	Fe_2O_3 (XRF)[a]	Grain size (d50)[b]
F1	2.68	4.06	6.49	19
F2	2.12	5.60	6.50	19
F3	2.31	4.57	6.03	19
F4	2.06	5.51	6.04	19
F5	2.62	13.74	9.30	48
F6	2.32	3.00	12.40	13
F7	2.11	3.11	8.32	41
S1	2.55	39.10	0.90	10
S2	2.76	40.62	0.53	9

Geopolymer				
Code	Liquid:precursor ratio paste	Water:precursor ratio paste	Sodium:precursor ratio paste	14 day strength (S) [MPa][c]
GF1	0.35	0.22	0.055	5.76
GF2	0.34	0.21	0.053	9.96
GF3	0.39	0.25	0.061	4.20
GF4	0.38	0.24	0.059	9.23
GF5	0.51	0.31	0.077	3.78
GF6	0.42	0.26	0.064	24.97
GF7	0.40	0.25	0.062	3.60
GS1	0.45	0.26	0.069	38.94
GS2	0.41	0.25	0.063	53.86

[a] XRF data are reported in Barnett et al. [2], except for F7 for which a representative average of this type of fly ash is taken from S&B Industrial Minerals [20]

[b] Grain size is represented here by d50; the Dutch fly ashes (F1–F4) are typically blends that generally do not vary significantly in grain size, as such, a typical value of d50 is given taken from a report from the fly ash provider [21]. The other grain size data are measured in this study or given by the providers

[c] 'S' is the compressive strength of the hardened paste at 14 days, with a method related error of 5 %

(10 M) (a similar approach was taken in Zhang et al. [26]). This approach introduces small differences in water:binder ratio and sodium/solid ratio, which will be considered when interpreting the results. Curing was done for 14 days at 20 °C and 98 % relative humidity. At 14 days strength was measured and the error related to the method (NEN-EN 206-1) is 5 %.

3 Methods

3.1 Solid state ^{29}Si-NMR

^{29}Si MAS NMR spectra were measured on an Agilent 300 MHz solid state NMR machine using a Bruker 7 mm probe tuned to 59.6 MHz for silicon and 300.15 MHz for protons. The magic angle spinning (MAS) speed was 6.25 kHz in all measurements. A Hahn-echo sequence was used applying an RF-field strength of 60 kHz. All spectra are referenced with respect to TMS (tetramethylsilane).

By deconvolving the ^{29}Si-NMR spectrum (Gaussean peak fitting aiming for the best fit with highest R^2-value), peaks occur at chemical shifts that are characteristic for different types of silicates. As such, by measuring the relative peak areas, a semi-quantitative estimate can be made of the relative amount of different types of silicates, classified according to the degree of polymerization and the number of aluminium nearest neighbours in the polyhedral adjacent to the Si

tetrahedron. For example, different framework silicates can be distinguished according to their characteristic chemical shifts: Q^4(4Al) [shift at −88 ppm]; Q^4(3Al) [shift at −90 ppm]; Q^4(2Al) [shift at −97 ppm]; Q^4(1Al) [shift at −104 ppm] and Q^4(0Al) [shift at −109 ppm], following the nomenclature $Q^n(m\text{Al})$, where *n* gives the polymerization degree of the silicon tetrahedra and *m* gives the amount of aluminium substitution per silicon tetrahedron. In this paper, the *relative* areas of only these aluminium–silicate peaks will be compared, giving a semi-quantitative indication of the *relative* amounts of these specific types of aluminium–silicates, each with their own Si:Al ratio. This approach is chosen based on the hypothes is that the amount of dissolvable glassy phases is not the dominant strength influencing factor, but rather the *ratio* of silica versus aluminium in the silicates which go into solution and as such the *ratio* that is available for geopolymerization.

It should be noted that no preassumption of peak assignment was made for the automated NMR deconvolutions because fly ashes are heterogeneous and not all phases can be predicted. The selection of best fit was based on the smallest error (highest R^2-value) between the fitted NMR spectrum and the original spectrum. This results in a large amount of deconvolved peaks, some of which may represent noise. However, only the relative areas of the peaks of framework silicates are considered [Q^4(nAl)], which means that the amounts of particular framework aluminium silicates are estimated relative to the total amount of framework aluminium silicates rather than to the total amount of phases in the precursor. This gives a more direct insight in the *ratio* of silicon to aluminium that really can go into solution. In that respect, noise or overlapping peaks of other phases do not significantly change the mutual comparison of the *relative* amounts of framework silicates. This approach has been verified by performing an alternative deconvolution using a fixed amount of predefined peaks, of which the outcome gave similar results when comparing only the relative areas of the chosen peaks (unpublished results). These findings were also shown in the study of Palomo and Fernández-Jiménez [13], where the different preassumptions before peak fitting did not have a major influence on the relative peak areas of aluminium–silicates, which were considered and compared in that paper.

An issue with solid state ^{29}Si-NMR is the reduced sensitivity due to paramagnetic broadening caused by iron. In addition, the presence of large quantities of iron results in difficulties for applying magic angle spinning due to its magnetic properties. Because the aim in this paper is to quantify deconvolved peaks, a high resolution data set is required. Therefore, particles containing magnetic properties related to iron, were removed from fly ash samples by strong magnets prior to NMR analysis. This significantly improved the signal to noise ratio of the NMR data. However, because the magnetic phases may be part of particles containing relevant aluminium–silicates, it is chosen to limit the comparative analysis of the relative peak areas in the discussion of this paper only to the samples that contained similar (low) amounts of iron and came from similar types of power plants. As such, the effect of eliminated iron on these samples is expected to be comparable, allowing relative comparison of the samples.

3.2 FT-IR spectroscopy

The FT-IR measurements in this paper were done using a Perkin-Elmer ATR-FT-IR Frontier with a diamond ATR crystal. The samples were manually grinded to achieve low fineness necessary for the measurements.

In principle, a measured FT-IR spectrum, is the combination of several peaks that overlap. By deconvolving the FT-IR spectrum, the relative areas of the peaks can give an estimate of the relative amount of particular types of atomic bonds and structures. This paper particularly focusses on the bands where aluminium–silicate species occur, which are of interest for geopolymerization (relevant wavenumbers between 650 and 1,350 cm^{-1}). Following baseline correction of all spectra to zero and normalisation of the spectra to enable comparison of individual samples, peak deconvolution using Gaussean peak fitting was performed. Maximum 6 peaks were fitted, similar to the deconvolutions done in this FT-IR spectral region by Criado et al. [5] and Zhang et al. [26]. The R^2-value of the combined fit of the deconvolved peaks to the original spectrum was kept above 0.995. The relative areas of the different deconvolved peaks were used as a semi-quantitative indication of the relative amounts of different atomic bonds and structures within a sample.

An indication for qualitative interpretation of aluminium–silicate species that have particular bonds and structures as found in FT-IR spectra, is given by Phair and van Deventer [14]: the broad peaks at around 1,000–1,100 cm^{-1} are attributed to T–O asymmetric stretching vibrations and represent the fusion of both Al–O and Si–O symmetric stretching. The lower wavenumbers can be viewed as related to a larger extent of aluminium incorporation into the silicate backbone [14]. It has been suggested that during geopolymerization, when initially silicates relatively rich in aluminium tend to be formed [9], these broad peaks shift to values around 900 cm^{-1} [14]. In general, symmetric and asymmetric stretching of the Si–O–Si bonds of the tetrahedra with n bridging oxygens are IR active in the 800–1,300 cm^{-1} range and with $n = 4, 3, 2, 1$, the bands are centered around 1200, 1100, 950 and 850 cm^{-1}, respectively. The lower wavenumbers result from replacing silicon with aluminium [10] and references therein).

For a (semi-)quantitative interpretation of the deconvolved peaks, peak assignment needs to be detailed further. Following the above remarks on aluminium-substitution, it can be argued that the aluminium- silicates may relate to deconvolved peaks from 1,300 to 800 cm^{-1}, with the most aluminium-rich silicates occurring at peaks down to 800 cm^{-1}. This, as well as the peak assignment of deconvolved peaks in this region as given in Zhang et al. [26] (Table 2), is taken into account for the interpretation of deconvolved peaks in the current paper. From Table 2, it can be seen that the higher wavenumber (1,000–1,300 cm^{-1}) peaks of the glassy (aluminium-poor) silicates as well as the lower wavenumber (800–900 cm^{-1}) peaks of the (aluminium-rich) silicates may overlap with the peaks of crystalline phases such as quartz and mullite. In between, the (900–1,000 cm^{-1}) peaks of glassy (medium aluminium) silicates have the least overlap with peaks of quartz and mullite. 'Active' bonds as indicated in Table 2 are those bonds that may dissolve in an alkaline medium, while 'inactive' bonds would not. In other words, between 900–1,000 cm^{-1}, the presence of 'active' bonds from the glassy (alkali-) aluminium-silicates is dominant, while in the higher (1,000–1,300 cm^{-1}) and lower bands (800–900 cm^{-1}), both 'active' bonds of aluminium-poor respectively aluminium-rich silicates as well as 'inactive' bonds of respectively quartz and mullite occur.

Table 2 Assignment of deconvolved bands as given in Zhang et al. [26] and references therein. The bonds that are considered for comparing precursors in this paper are indicated in bold

Position [cm^{-1}]	Assignment	Classification of bonds
>1184	Asymmetric stretching of Si–O–Si in silicate framework structures, Q^4	Inactive
1139–1161	Asymmetric stretching of (Si,Al^{IV})–O–Si in mullite or mullite-like structures	Inactive
1085–1092	Asymmetric stretching of (Si,Al^{IV})–O–Si in glass (may partially overlap with mullite and quartz)	Active
997–1011	**Asymmetric stretching of (Si,Al^{IV})–O–Si in amorphous glasses, could be composed of higher Al concentration**	**Active**
900–915	**Stretching of Si–O–(M, Me, Fe) where M is an alkali metal or Me is an alkali-earth metal, or Si–OH**	**Active**
795–814	Symmetric stretching of Si–O–Si in quartz, and stretching Al^{VI}–O in mullite-like structures	Inactive
692–730	Symmetric stretching of Al–O in Si(Al^{IV})–O–Al^{IV} linkages	Active
612–618	Bending of O–Al^{IV}–O in mullite or mullite-like structure	Inactive
543–554	Symmetric stretching of Al–O–Si in mullite or mullite like structures	Inactive
<461–465	Bending of Si–O–Si and O–Si–O in Si-rich glass or quartz	Inactive

4 Results

4.1 Solid state ^{29}Si-NMR

In Fig. 1, the ^{29}Si-NMR spectra of four selected fly ash samples with similar iron content and of their geopolymers are shown. It is seen that the fly ash samples have similar overall spectra with the dominant part around −110 ppm, while the geopolymer spectra show more distinct differences, with the spectrum shifting towards −100 and −90 ppm.

The deconvolved ^{29}Si-NMR spectrum of fly ash F1 and its respective geopolymer paste GF1 is presented as a representative example for the source materials in Fig. 2. In this example it is seen that the overall

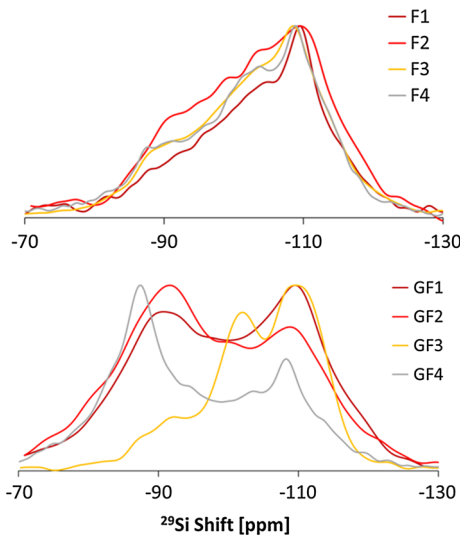

Fig. 1 ^{29}Si-NMR spectra of four selected fly ash samples and their respective geopolymers

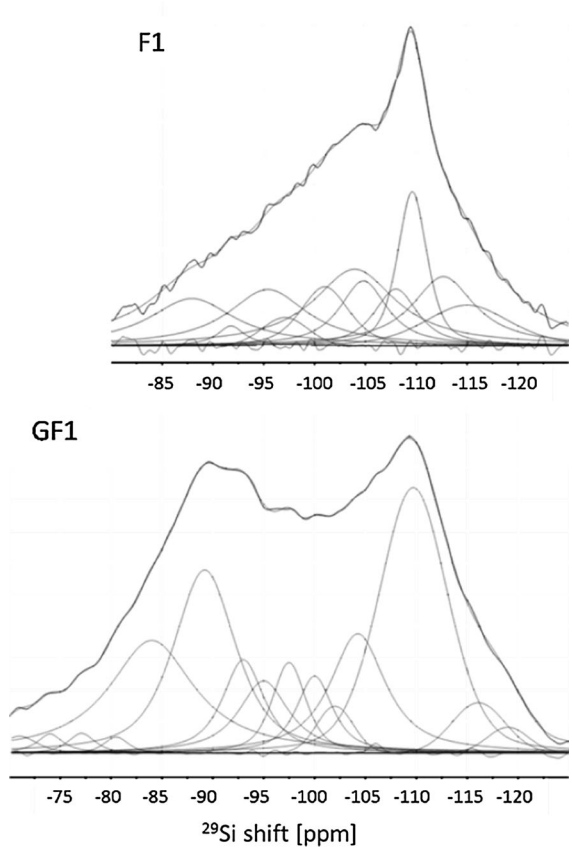

Fig. 2 Deconvolved ^{29}Si-NMR spectrum of fly ash F1 and its geopolymer paste GF1

spectrum for the fly ash has more significant peaks at the shifts representing low aluminium framework silicates, namely Q^4(0Al) (−109 ppm) and Q^4(1Al) (−104 ppm), while for the corresponding geopolymer an increase is seen in the peaks representing framework silicate phases with medium to high amounts of aluminium incorporated, namely Q^4(2Al) (−97 ppm), Q^4(3Al) (−90 ppm) and Q^4(4Al) (−88 ppm). This shows that the fly ash has reacted to form more alumina-rich silicate phases.

Table 3 shows the relative areas of peaks as detected by deconvolution of ^{29}Si-NMR spectrum of the different source materials. It is evident that the relative amounts of the four types of framework aluminium-silicates vary for the different fly ashes. It is noted that after deconvolution, the main peak shifts represent framework aluminium-silicate phases (Q^4) and virtually no peaks were found at shifts representing chain (Q^2) or sheet silicates (Q^3). Because the amounts of the latter were so small or non-existing, they have been left out of the comparative analysis of relative areas of deconvolved peaks.

4.2 FT-IR spectroscopy

Figure 3 shows the FT-IR spectra of all fly ash and slag samples and their corresponding geopolymer pastes. For the fly ash source material, a broad peak occurs around ∼1,000 cm^{-1}, with a small hump at lower wavelengths around 900 cm^{-1}. The spectra of the slag samples are significantly different with their broad peak occurring around 900 cm^{-1}, where the fly ash samples only have a small hump.

After geopolymerization, the main characteristic in all geopolymers is that the band associated with T–O stretching vibrations (∼1,000 cm^{-1}) as seen in the precursors shifts to values around ∼900 cm^{-1} and becomes sharper. The magnitude of the shift is thought to be determined by the aluminium atom content per unit of formula: it moves to lower wavelengths with an increase in the content per unit of the tetrahedrally positioned aluminium atom in the silicates. Moreover the substitution of a Si^{4+} for an Al^{3+} causes a reduction of the T–O–T angle and therefore the appearance of the signal at a lower frequency is due to smaller bonding force and the fact that Al–O bond is longer than Si–O bond [14].

Table 3 FT-IR and NMR quantification results obtained in this study for 9 different source materials and their corresponding geopolymer pastes

	FT-IR	Relative area [%] of FT-IR peak for average peak centre [cm^{-1}]						NMR	Relative area (%) of NMR peak for chemical shift				
Source material	Peak name and location [cm^{-1}]	724	842	908	947	1,066	1,162	Chemical shift [ppm]	Q^4(4Al) −88	Q^4(3Al) −90	Q^4(2Al) −97	Q^4(1Al) −104	Q^4(0Al) −109
F1	Relative peak area [%]	52.7	0.0	2.5	10.4	30.0	4.5	Relative peak area [%]	17.2	2.3	22.3	36.5	21.8
F2		53.9	0.0	2.7	13.2	27.9	2.4		9.0	10.0	28.0	21.0	31.0
F3		57.9	0.0	2.5	11.3	24.9	3.4		21.5	0.0	14.2	5.9	58.4
F4		58.9	0.0	2.3	17.8	17.0	3.9		12.0	0.0	26.1	35.0	27.0
F5		46.7	0.0	0.7	18.1	26.3	8.2		–	–	–	–	–
F6		55.8	0.0	1.3	27.7	11.6	3.5		–	–	–	–	–
F7		64.3	0.0	1.8	17.3	12.9	3.7		–	–	–	–	–
S1		20.5	31.8	3.5	44.3	0.0	0.0		–	–	–	–	–
S2		21.4	32.0	1.4	45.2	0.0	0.0		–	–	–	–	–
Geopolymer	Peak location [cm^{-1}]	683	835	882	962	1,056	1,158	Chemical shift [ppm]	−88	−90	−97	−104	−109
GF1	Relative peak area [%]	54.0	0.0	2.2	32.3	8.5	3.0	Relative peak area [%]	19.0	6.6	15.8	14.0	26.0
GF2		49.3	0.0	7.2	30.3	10.6	2.6		30.6	18.4	27.4	2.7	11.6
GF3		52.3	0.0	10.8	24.8	9.7	2.4		1.3	0.0	2.7	35.1	60.8
GF4		51.2	0.0	7.6	28.1	10.6	2.5		39.7	0.0	20.2	18.9	21.2
GF5		32.7	0.0	13.7	43.0	5.4	5.3		–	–	–	–	–
GF6		35.3	0.0	12.7	30.0	21.1	0.9		–	–	–	–	–
GF7		47.7	0.0	10.1	29.5	9.6	3.1		–	–	–	–	–
GS1		35.3	18.6	10.0	11.1	24.7	0.3		–	–	–	–	–
GS2		39.3	17.6	6.1	9.9	26.6	0.6		–	–	–	–	–

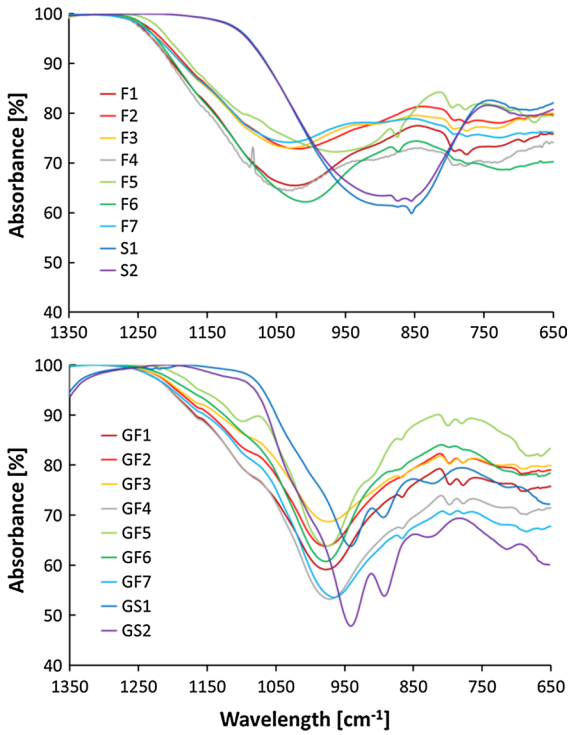

Fig. 3 FT-IR spectra of the source materials and their corresponding geopolymer pastes

Figure 4 shows the deconvolution of the FT-IR spectra of fly ash F2 and slag S1 and their respective geopolymer pastes. As a representative example, deconvolution of the broad $\sim$1,000 cm^{-1} peak of fly ash F2 (Fig. 3), shows 4 deconvolved peaks, with a significant peak at the aluminium-poor silicate side of the spectrum (>1,000 cm^{-1}). In contrast, for the geopolymer paste of F2 (GF2), a significant peak in the band of silicates with a higher aluminium incorporation is seen (900–1,000 cm^{-1}). As a second representative example, the main peak centra for slag S1 occur in the medium to high aluminium-silicate band (Fig. 4). Upon geopolymerization, the peaks become sharper compared to those of the precursors (Fig. 4). It should be noted here that slag contains a significant amount of calcium, which is mostly incorporated in the aluminium-silicates, as such possibly distorting the T–O–T angle and affecting the T–O bonding force, consequently lowering the frequency of the aluminium-silicate peaks. In general, for all source materials, after geopolymerization, the deconvolved peaks of the low aluminium-silicates tend to broaden and lower peak height, while those of the medium to high aluminium-silicates tend to become sharper and increase peak height. This is also reflected in the relative areas of the peaks (Table 3).

5 Discussion

For the interpretation and discussion, the results are presented as a series of graphs, where relevant variables in the source material (precursor) and geopolymer mix are plotted versus strength.

On Figs. 5 and 6 it is seen that the water:precursor ratio and the total sodium:precursor ratio do not show a systematic trend with strength. Grain size shows a variable trend with strength: for small grain sizes, strength varies significantly with very small variations in grain size, while for larger grain sizes, strength shows very little variations with size (Fig. 7). Therefore it is hard to use grain size alone as a uniform indicator of the potential for geopolymerization. The Si:Al ratio hints towards a trend where a higher Si:Al in some cases is linked to higher strength (Fig. 8). This may be related to the fact that the amount of aluminium versus silicon in a structural silicate unit has an influence on the ability of the aluminium-silicate bonds to dissolve and as such on the available aluminium versus silicon to form reaction products. However, the reflection of this in the Si:Al ratio relation with strength may be blurred because this ratio is based on *average* bulk aluminium and silicon contents regardless of the variations that exist in aluminium-silicate phases and bonds within one precursor.

With solid-state ^{29}Si-NMR, direct evaluations can be made of the type of aluminium-silicate bonds. It should be noted that framework silicates can be both glassy (reactive) as well as crystalline (non-reactive). Regions that are most prone to have an overlap of crystalline and non-crystalline phases are around the Q4(3Al) shift (includes mullite) and around the Q4(0Al) shift (includes quartz). Therefore, for an evaluation with strength, only the Q4(2Al) and the Q4(4Al) shifts are presented in a graph. On Fig. 9 it is seen that an increasing relative amount of (medium-) aluminium silicates Q^4(2Al) corresponds to an increasing strength. In contrast, an increasing amount of aluminium-silicates rich in aluminium Q^4(4Al) corresponds to a decreasing strength. It is noted that comparable trends have been observed by Fernández-

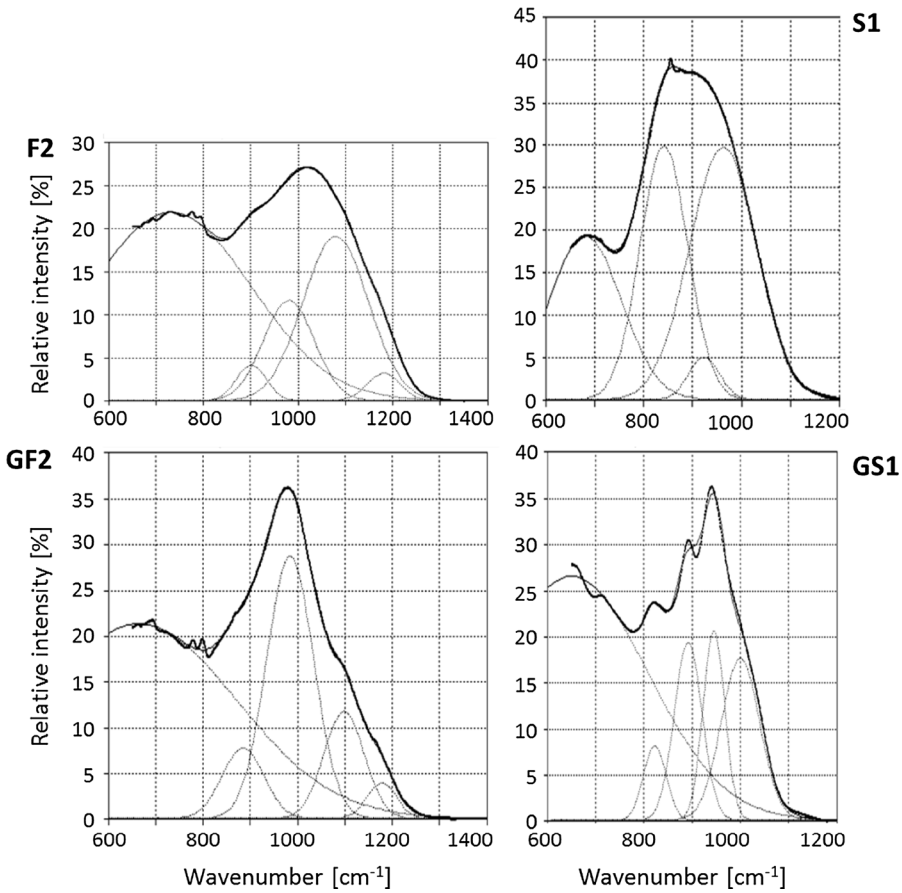

Fig. 4 Deconvolved FT-IR spectra of fly ash F2 and S1 and their corresponding geopolymer paste GF2 and GS1

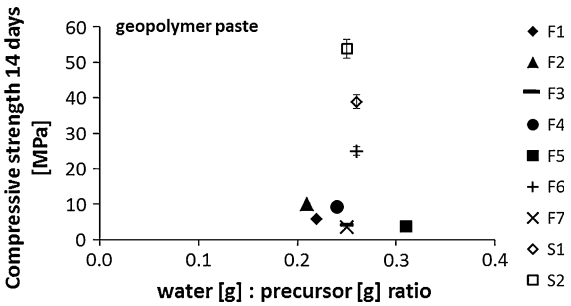

Fig. 5 Graph showing variations in water:precursor ratio of the geopolymer paste versus 14 days geopolymer paste compressive strength

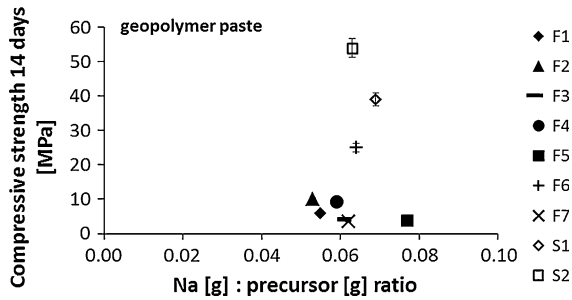

Fig. 6 Graph showing variations in natrium:precursor ratio of the geopolymer paste versus 14 days geopolymer paste compressive strength for different precursors (see legend)

Jiménez et al. [9] and also by the current authors by using ^{27}Al-NMR for evaluating aluminium-coordination (unpublished results).

The above observed trends for Q^4 silicate networks in precursors with geopolymer strength, are explained as follows. The fastest way to form 3D (Q^4) silicate networks is to incorporate aluminium atoms as there is an energetic preference for bonding between unlike atoms within an aluminium-silicate framework, meaning that Si–O–Al bonds are generally preferred. Therefore, a minimum amount of aluminium in the

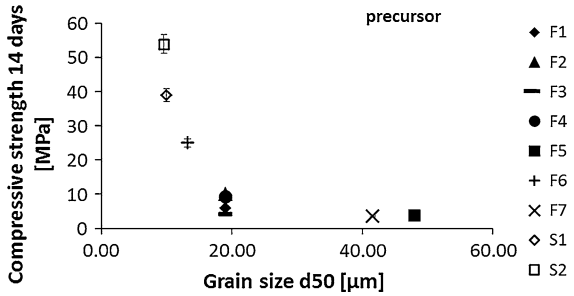

Fig. 7 Graph showing variations in grain size [d50] of the precursor versus 14 days geopolymer paste compressive strength for different precursors (see legend)

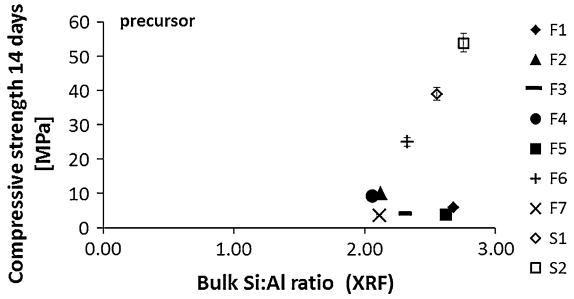

Fig. 8 Graph showing variations in bulk Si:Al ratio of the precursor versus 14 days geopolymer paste compressive strength for different precursors (see legend)

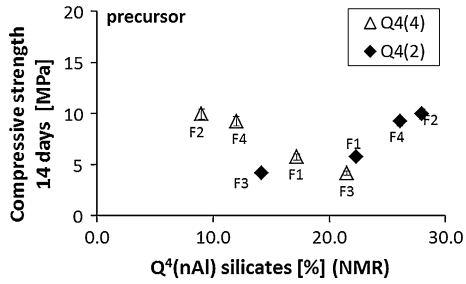

Fig. 9 Graph showing variations in the relative areas (%) of two deconvolved peaks [representing relative amounts of $Q^4(2Al)$ and $Q^4(4Al)$ silicates] of the precursor versus 14 days geopolymer paste compressive strength for different precursors (indicated next to data points). Due to paramagnetic broadening caused by iron in the ^{29}Si NMR signal, only NMR data are shown for samples with similar and low amounts of iron (F1-F4)

silicates that can be dissolved from the source material is required to easily form the strong 3D reaction products. However, in diluted alkaline dissolution experiments, silicates containing a lot of aluminium

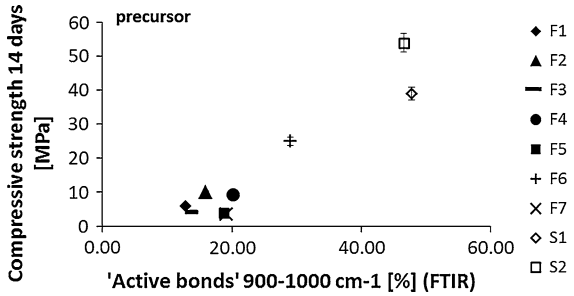

Fig. 10 Graph showing variations in the relative amounts of 'active bonds' of the precursor (in the 900–1,000 cm^{-1} FT-IR region) versus 14 days geopolymer paste compressive strength for different precursors (see legend)

have been observed to dissolve slower than aluminium-poor silicates [11, 22, 24]. Also, it has been stated previously that the high amount of aluminium available speeds up the gelation and formation of aluminium–silicates so much, that precipitation on the source material slows down the further dissolution [9], which eventually may lead to geopolymers with lower mechanical performance. This would imply that the medium-aluminium–silicate phases $Q^4(2)$ are ideal as they still dissolve relatively easy because they do not contain too much aluminium, but they also contain enough aluminium to rapidly form the 3D strength enhancing aluminium–silicate networks. Alternatively, the $Q^4(4)$ containing a lot of aluminium eventually tends to dissolve slower and decrease strength development. In other words, in pure NaOH activated systems, the aluminium–silicate structure not only influences the dissolution rate, but also the amount of aluminium that is released with respect to silicon for the precipitation of strong Q^4, aluminium–silicates, which are indeed initially enriched in aluminium as seen from the peak shifts upon geopolymerization (chapter 4).

For interpreting the FT-IR results with respect to geopolymer paste strength, it is chosen to look at the bands where predominantly peaks of 'active' bonds occur (not disturbed by 'inactive' bonds), which correspond to bands where peaks occur from the aluminium–silicates with medium amount of aluminium and alkalis (see methods paragraph and Table 2). For this, the sum is taken of the relative amounts of FT-IR deconvolved peaks between 900 and 1,000 cm^{-1}. Similar to what is seen with NMR, increasing relative amounts of these glassy 'medium' aluminium–silicates corresponds to increasing

strengths (Fig. 10). It is noted that the precursors with the highest relative amount of reactive 'medium' aluminium silicates are fly ash (F6) with a high amount of iron, and two slags (with a high amount of calcium). Both iron and calcium (which may be substituted in the aluminium–silicates) are known to have a positive effect on geopolymerization.

In this study it is avoided to incorporate crystalline phases like mullite and quartz when comparing FT-IR as well as NMR results. The effect of crystalline phases in a precursor is that they result in a relatively lower amount of glassy phases that can be dissolved. In that respect they can form an important characteristic of the precursor. Nevertheless, as shown above, the dominant factor is not necessarily the total quantity of what goes into solution, but rather the 'quality', i.e., the *ratio* of aluminium versus silicon goes into in solution. For example, fly ashes with very little mullite and rich in glass indeed easily go into solution, but they may not form the required strong reaction products if not enough aluminium is dissolved [24]. Of course, it is likely there may be a minimum total amount of glass needed that goes into solution, but if the glassy phases do not have the appropriate silicon to aluminium ratio, this will not enhance geopolymerization.

The methods in this study show a way of assessing the relative amounts of specific types of silicates, which go into solution and as such affect the resulting dissolved Si:Al ratio. In other words, the dissolved Si:Al ratio is dependent on the original structure of the aluminium–silicate glass in the precursor rather than on the total amount of glass. In other words, FT-IR and NMR are used to assess the relative amounts of phases that (1) are expected to dissolve and are the least influenced by overlapping peaks of non-reactive crystalline silicates, and (2) are key in determining the Si:Al ratio into solution.

The trend between geopolymer strength and the relative amount of particular aluminium–silicate types in the source material as measured using FT-IR as well as ^{29}Si-NMR, has the potential to be the basis for a successful screening tool for assessing the quality of secondary resource materials for high-performing geopolymers. ^{29}Si-NMR has the advantage that it measures silicate structures over longer distances than just one atomic bond and as such gives more accurate and quantifiable information about polymerization than FT-IR, the latter measuring only the bond between two atoms, while not 'seeing' its longer range neighbours. Although FT-IR is therefore less straightforward for aluminium-silicate phase determination, it has the advantage that it is much faster and less elaborate than ^{29}Si-NMR, and not sensitive for iron in source materials. So, provided more of this type of analyses are done to validate the observed trends, FT-IR has the potential to be a quick and user-friendly quality control tool of secondary resources for geopolymer applications like concrete.

It should be emphasized here again that the aluminium-incorporation in silicates of the precursors not only affects dissolution rate but also the ratio of aluminium with respect to silicon that goes into solution and therefore the rate of 'precipitation' and eventually the amount of aluminium-incorporation of the reaction product. The Si:Al ratio of the reaction products can also be evaluated using FT-IR and NMR as shown in Chapter 4. Knowledge on this aspect can help to steer the amount of additional silicate (and/or aluminate) in the activator solution that would help to enhance strength development, for example by using waterglass in addition to NaOH. Waterglass was not used here as the aim was to look solely at the influence of the precursor.

Lastly, the fact that such a clear trend has been observed for 9 significantly different source materials (fly ash as well as slag), hints that the aluminium incorporation in silicates of the source materials predominates above other strength influencing parameters of the precursors such as particle size, shape, particle porosity, water demand etc. However, future refinement for screening of source materials may involve the correction of the above observed trend for these other parameters (see for example [26]).

6 Conclusion

Deconvolution of FT-IR spectra of 9 precursors (fly ash and slag) and their geopolymers allowed to estimate the relative amounts of different aluminium-silicate types. In order to evaluate the potential of a precursor, a simple geopolymer system based on NaOH activation was used to investigate the precursor's ability to dissolve and form particular 3D networks at a time slice of 14 days. A clear trend is observed for both NMR and FT-IR results: the precursors containing a higher amount of 'active bonds', predominantly from silicates with a medium amount of aluminium and alkalis incorporated in their

3D framework, tend to result in higher paste strengths. This trend can be related to the influence of the ratio of silica to aluminium in the glassy silicates on the ability to dissolve as well as to form geopolymer reaction products.

^{29}Si-NMR as a measurement tool has the advantage of enabling detailed identification of different types of aluminium-silicate species. However, the disadvantage of NMR is its sensitivity to the presence of iron, which may hinder the acquisition of reliable spectra that can be deconvolved. The advantage of FT-IR is that it is not hindered by iron content and gives faster measurements than ^{29}Si-NMR, and even though the FT-IR deconvolutions are less detailed with respect to aluminium-silicate phase identification, the calculated relative areas of the medium aluminium-silicate peaks in fly ash as well as slag do give a clear trend with strength. Due to its relatively quick measurements, (semi-)quantitative FT-IR has therefore future potential to be particularly useful as screening tool for efficient precursor quality control, geopolymer design and optimization.

Acknowledgments The research leading to the results in this paper has received funding from the European Union FP7/2007-2013 programme (GA n°285463). Support of NWO for the 'Solid state NMR facility for advanced materials science' in Nijmegen is acknowledged. Vliegasunie BV, RockTron International Limited, West Burton Power Station, Ecocem Materials Limited, Hanson UK, Queen's University Belfast and the National Technical University of Athens are acknowledged for providing the samples. The UK samples were selected based on the work described in Barnett et al. [2], carried out at Liverpool University in the Carbon Trust funded project 0911-0252.

References

1. Barbosa VFF, MacKenzie KJD, Thaumaturgo C (2000) Synthesis and characterization of materials based on inorganic polymers of alumina and silica: sodium sialate polymers. Int J Inorg Mater 2:309–317
2. Barnett S, Hadjierakleous Q, Soutsos M (2011) Alkali activated binders from UK fly ashes. In: Proceeding of the 31st cement and concrete science conference, Imperial College London, London, 12–13 Sept 2011
3. Chen-Tan NW, Van Riessen A, Ly CV, Southam DC (2009) Determining the reactivity of a fly ash for production of geopolymer. J Am Ceram Soc 92:881–887
4. Chindaprasirt P, Chalee W, Jaturapitakkul C, Rattanasak U (2009) Comparative study on characteristics of fly ash and bottom ash geopolymers. Waste Manag 29:539–543
5. Criado M, Fernández-Jiménez A, Palomo A (2007) Alkali activation of fly ash: effect of the SiO2/Na2O ratio Part I: FT-IR study. Micropor Mesopor Mat 106:180–191
6. Duxson P, Provis JL (2008) Designing precursors for geopolymer cements. J Am Ceram Soc 91:3864–3869
7. Duxson P, Fernandez-Jimenez A, Provis JL, Lukey GC, Palomo A, Van Deventer JSJ (2007) Geopolymer technology: the current state of the art. J Mater Sci 42:2917–2933
8. Fernández-Jiménez A, Palomo A (2003) Characterisation of fly ashes. Potential reactivity as alkaline cements. Fuel 82:2259–2265
9. Fernández-Jiménez A, Palomo A, Sobrados I, Sanz J (2006) The role played by reactive alumina content in the alkaline activators of fly ashes. Micropor Mesopor Mat 91:111–119
10. Mashal K, Harsh JB, Flury M, Felmy AR (2005) Analysis of precipitates from reactions of hyperalkaline solutions with soluble silica. Appl Geochem 20:1357–1367
11. Nugteren HW (2010) Secondary industrial minerals from coal fly ash and aluminium anodizing waste solutions. Dissertation, Technical University of Delft (the Netherlands)
12. Nugteren HW, Butselaar-Orthlieb VCL, Izquierdo M (2009) High strength geopolymers produced from coal combustion fly ash. Global NEST J 11:155–161
13. Palomo A, Fernández-Jiménez A (2007) Nature of alkali aluminosilicate polymers; a ^{29}Si MAS-NMR approach. In: Proceeding of the '3rd international conference alkali activated materials-research, production and utilization', Prague, 509–522
14. Phair J, van Deventer JSJ (2002) Effect of the silicate activator pH on the microstructural characteristics of waste-based geopolymers. Int J Miner Process 66:121–143
15. Provis JL, Duxson P, Lukey GC, van Deventer JSJ (2005) Statistical thermodynamic model for Si/Al ordering in amorphous aluminosilicates. Chem Mater 17:2976–2986
16. Provis JL, van Deventer JSJ (2007) Geopolymerization kinetics. 1. In situ energy-dispersive X-ray diffractometry. Chem Eng Sci 62:2309–2317
17. Provis JL, van Deventer JSJ (2007) Geopolymerization kinetics. 2. Reaction kinetic modelling. Chem Eng Sci 62:2318–2329
18. Provis JL, van Deventer JSJ (2009) Geopolymers: Structure, processing, properties and industrial applications. Woodhead Publishing Limited, Cambridge
19. Rahier H, Wastiels J, Biesemans M, Willem R, Van Assche G, Van Mele B (2007) Reaction mechanism, kinetics and high temperature transformations of geopolymers. J Mater Sci 42:2982–2996
20. S&B Industrial Minerals SA (2012) Sustainable, innovative and energy-efficient concrete, based on the integration of all-waste materials: SUS-CON deliverable D3.1—samples identification cost estimates parameters affecting reactivity, Report FP7 proposal number 285463 SUS-CON
21. Saraber AJ, Vissers JLJ (2006) Invloed van poederkoolvliegas op de verwerkbaarheid van beton. Kema Rapport 50431005.CL.5 04P5.2.4. Arnhem
22. Songpiriyakij S, Kubprasit T, Jaturapitakkul C, Chindaprasirt P (2010) Compressive strength and degree of reaction of biomass- and fly ash-based geopolymer. Constr Build Mater 24:236–240
23. van Deventer JSJ, Provis JL, Duxson P (2012) Technical and commercial progress in the adoption of geopolymer cement. Miner Eng 29:89–104

24. Valcke SLA, Sarabèr AJ, Pipilikaki P, Fischer HR, Nugteren HW (2013) Screening coal combustion fly ashes for application in geopolymers. Fuel 106:490–497
25. Williams RP, Van Riessen A (2010) Determination of the reactive component of fly ashes for geopolymer production using XRF and XRD. Fuel 89:3683–3692
26. Zhang Z, Wang H, Provis JL (2012) Quantitative study of the reactivity of fly ash in geopolymerization by FT-IR. J Sustainable Cement-Based Mater 1:154–166